Inorganic Chemistry

Communication

pubs.acs.org/IC

Flash and Continuous Photolysis Kinetic Studies of the Iron–Iron Hydrogenase Model (μ-pdt)[Fe(CO)$_3$]$_2$ in Different Solvents

Jon Marhenke,[†] Agustin E. Pierri,[‡] Melanie Lomotan,[§] Peter L. Damon,[§] Peter C. Ford,[‡] and Carmen Works*[,§]

[†]Department of Physical Sciences, Butte College, Oroville, California 95965, United States

[‡]Department of Chemistry and Biochemistry, University of California, Santa Barbara, Santa Barbara, California 93106-9510, United States

[§]Department of Chemistry, Sonoma State University, Rohnert Park, California 94928-3609, United States

Supporting Information

ABSTRACT: Flash and continuous photolysis studies of (μ-pdt)[Fe(CO)$_3$]$_2$ under excess CO were conducted in coordinating and noncoordinating solvents. The back-reaction of CO with the photoproduct showed second-order kinetics with k_{CO} values of 1.0×10^8, 3.4×10^6, 1.2×10^6, and 0.90 M^{-1} s^{-1} in hexanes, benzene, toluene, and THF, respectively. These data indicate a solvent-coordinated intermediate as one photoproduct, but other long-lived species were also apparent.

The reversible oxidation of H_2 is catalyzed by hydrogenase, and CO is a competitive inhibitor for hydrogen activation.[1−5] The active site of iron–iron hydrogenase (the "H-cluster") is a dinuclear iron complex with a 1,3-dithiolate-like bridge and CO and CN^- ligands.[2] The H-cluster is tethered to a ferridoxin-type cluster that functions as an electron source. Hydrogen is believed to bind at the H-cluster, in the active site of the enzyme.[2] The organometallic core has inspired the synthesis of several structural and functional models of the enzyme active site with bridging 1,3-propanedithiolate (pdt).[6]

The cyano and phosphorus hydride versions of the models participate in H/D exchange but only in the presence of sunlight, suggesting that they have potential as photoactive catalysts.[8] These molecules are better described as models for the CO-inhibited form of the H-cluster. Photolysis reverses this inhibition in the biological system.[9] Among the models previously reported, (μ-pdt)[Fe(CO)$_3$]$_2$ (**1**) has received the most attention and has been shown to be photochemically active, with photolysis resulting in cleavage of an Fe–CO bond.[6,9−13]

Recent studies have been concerned with characterizing the photochemistry and photoproducts of **1**, but little attention has focused on the reaction dynamics of these photoproducts with CO, which are important in determining the catalytic reactivity. A study by Hunt et al using ultrafast time-resolved IR (TRIR) spectroscopy demonstrated the formation of solvent adducts in alkane and nitrile solvents within 30–60 ps and showed that, in a mixed heptane/heptyl nitrile solvent, the initially formed alkane adduct was displaced on a nanosecond time scale by the nitrile to form a longer-lived nitrile complex.[10] Such studies are important in comprehending the chemistry of these models and give insight into the enzymatic reactions. Another aspect of the models is that the synthetic scaffold provides opportunities for derivatives that may serve as water-soluble photochemical CO-releasing molecules.[14] CO is a physiological signaling molecule, and precursors that can release CO in a controlled manner may have therapeutic applications.[15]

Described here are longer-time-scale kinetic studies for the reaction of species produced by photolysis of **1** with excess CO in various solvents. Both laser-flash and continuous photolysis were used to generate reactive intermediates depending on the solvent system.

The optical spectrum of **1** shows intense peaks ($\varepsilon \sim 12\,600$ M^{-1} cm^{-1}) at 345 nm in toluene and at 327 nm in tetrahydrofuran (THF), and this band has been assigned as HOMO−2 → LUMO [Fe(t_{2g}) → Fe(σ^*)].[12] There is also a less intense broad absorbance around 450 nm ($\varepsilon \sim 10^3$ M^{-1} cm^{-1}) assigned as a d → σ^* metal-to-ligand charge-transfer (MLCT) transition for the $Fe_2S_2(CO)_6$ analogue[13] and HOMO → LUMO [Fe(σ) → Fe(σ^*)] for **1** in acetonitrile.[12] The IR spectrum shows three to five peaks in the carbonyl region depending on the solvent.[6] When a solution of **1** is irradiated with 355 nm light, the optical and IR spectra change as a new species forms.[6,10−13] IR spectral changes show depletion of the parent peaks and growth of peaks at lower frequency, consistent with the formation of a solvent adduct.[10] The difference IR spectrum of **1** in THF is shown in the Supporting Information (SI), and the difference IR spectrum of **1** in toluene was published previously.[6] When a toluene solution of **1** was irradiated under excess CO, no net changes were observed in the optical or IR spectra, suggesting solvent-dependent thermal reactivity of the photoproduct. That is, in weakly coordinating hydrocarbon solvents, reaction of the photoproduct with CO to regenerate **1** appears to be too fast to observe using conventional UV–vis spectroscopy. Notably, hydrophobic amino acid residues of the enzyme create a pocket around the H-cluster.[16] Furthermore, one of those residues, phenylalanine, is aromatic.

When a THF solution of **1** under CO was irradiated with the 365 nm output of a hand-held UV lamp, a bleach of λ_{max} at 327 nm was observed that coincided with an absorbance increase at

Received: July 18, 2011
Published: October 28, 2011

   dx.doi.org/10.1021/ic201523r | *Inorg. Chem.* 2011, 50, 11850–11852

400 nm. The slow thermal regeneration of the 327 nm peak was monitored as a function of time. The resulting kinetic traces were fit to generate observed first-order rate constants. The linear plot of k_{obs} versus [CO] (Figure 1) indicates a

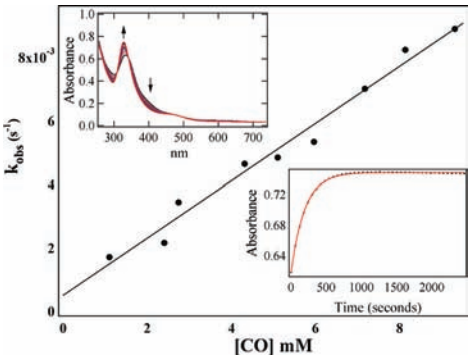

Figure 1. CO concentration rate dependence for the back-reaction of the photoproduct of **1** with CO in THF at 23 °C.[17] The slope (k_{CO}) is 0.92 M^{-1} s^{-1}. Inset: (top) temporal spectral changes for reaction of the photoproduct with CO (2.7 mM); (bottom) absorbance changes as a function of time monitored at 327 nm (black dots) and the monoexponential fit (red line).

second-order reaction, first order in the photoproduct and CO. The slope represents the second-order rate constant k_{CO} and is 0.90 M^{-1} s^{-1}, and the y intercept, (5.2 ± 3.0) × 10^{-4} s^{-1}, is not significantly different from zero. Similar behavior was observed in acetonitrile. These observations are consistent with the reversible photolabilization of CO from **1** to give a solvent-coordinated intermediate that slowly back-reacts to re-form **1**, as shown in Scheme 1. The photochemical reaction was also

Scheme 1. Proposed Photoreactivity of 1 in THF and Excess CO

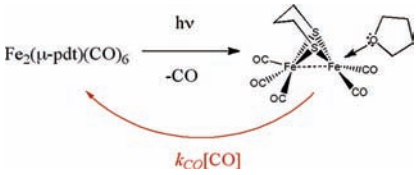

monitored by IR in both THF (Figure S-1) and acetonitrile,[6,10] and the spectral changes, specifically the formation of peaks at lower frequencies, are consistent with density functional theory (DFT) calculations, confirming the formation of a solvent adduct.[10] In addition, the reaction kinetics of the photoproducts with CO were monitored in the IR (Figure S-2).

Although the back-reaction with CO was sufficiently slow in THF, this was not the case in hydrocarbon solvents, where it was necessary to use laser-flash photolysis techniques. These involved excitation with 355 nm pulses (~10 ns pulse length) from a Nd:YAG laser and monitoring absorbance changes.[14] Figure 2 shows photolysis-induced changes in absorbance at 400 nm for a solution of **1** in toluene under excess CO. The disappearance of the transient signal was fit with a monoexponential function to yield k_{obs}. Figure 2 is a plot of k_{obs} as a function of [CO], and the linear fit gives a k_{CO} value of (1.09 ± 0.06) × 10^6 M^{-1} s^{-1}. There did remain a residual difference from the initial absorbance that persisted after the CO-dependent decay finished, although any such residual

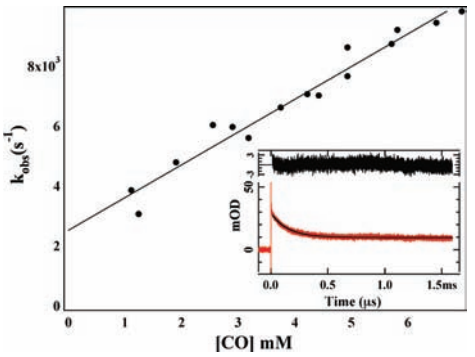

Figure 2. Plot of k_{obs} versus [CO] for the reaction of transients generated by flash photolysis of (μ-pdt)[Fe(CO)$_3$]$_2$ with CO in toluene at 23 °C. Inset: kinetic trace (red) collected at 3.18 mM CO and monitored at 400 nm. The fit to this trace is shown in black.

diminished on longer time scales than the laser-flash experiment.

The linear relationship between k_{obs} and [CO] again suggests photolabilization of CO and recoordination but with a back-reaction rate of more than 6 orders of magnitude faster than that observed in THF or acetonitrile. However, for the toluene experiments, there is a significantly nonzero y intercept [(2.5 ± 0.3) × 10^3 s^{-1}]. This observation is consistent with a mechanism that has two pathways for photoproduct decay, as shown in Scheme 2 ($k_{obs} = k_1 + k_{CO}[CO]$). One is the reaction

Scheme 2. Proposed Reactivity of 1 in Aromatic Solvents

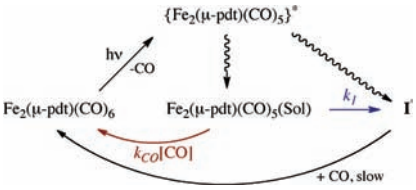

with CO to re-form **1**, while the second is CO-independent and leads to another, longer-lived species. Notably, the magnitude of the residual nonzero absorbance changes in the toluene experiments is a function of the CO concentration, decreasing substantially with increasing [CO] (Figure S-3). However, some residual was observed even at the highest [CO] studied, an observation that might be explained by the prompt formation of some of the second transient **I′** in competition with relaxation of the initial excited states to the thermalized solvated intermediate Fe$_2$(μ-pdt)(CO)$_5$(Sol). While the residuals faded on a longer time scale when the solution was left in the dark, some permanent photodecomposition was evident after repetitive excitation with the laser (Figure S-4). Some choices for this intermediate include a CO-bridged species or a pseudo dimer formed between the hexacarbonyl and solvent adduct, but thus far there is no structurally revealing experimental data on our time scales or ultrafast time scales.[10]

Flash photolysis studies were also carried out in benzene and hexanes solutions, and the k_{CO} values were even larger than that measured in toluene, 3.4 × 10^6 and 1.0 × 10^8 M^{-1} s^{-1}, respectively. However, the behaviors of these two solvents differed, with a large nonzero intercept for the benzene data (Figure S-5; k_1 = 1.6 × 10^4 s^{-1}) but not for the hexanes data (Figure S-6). It is not clear why the second reaction pathway is

dx.doi.org/10.1021/ic201523r | Inorg. Chem. 2011, 50, 11850–11852

evident only in the aromatic solvents, although one could argue that the uncertainty in the hexanes plot intercept ($\pm 1 \times 10^4$ s^{-1}) is comparable to the k_1 values seen for the aromatic solvents. Alternatively, the aromatic π system may have some special and interesting interaction that enhances the formation and stabilization of **I′**.

Photolysis of the $Fe_2S_2(CO)_6$ cluster in a Nujol matrix generated different photoproducts depending on the wavelength of irradiation.[11] CO was labilized when irradiated at wavelengths below 420 nm and that other photoproducts were generated with wavelengths greater than 420 nm. Furthermore, Kunkely and Vogler[13] showed that the nonthiol-bridged analogue formed higher-order clusters upon 436 nm photolysis, although the spectral changes were very similar to what we have observed for CO loss.[6] To address the possibility of cluster formation, we carried out laser-flash photolysis in a toluene solution using varied iron concentrations but constant [CO] and measured the residual changes in absorbance. No variation in residual absorbance changes were seen, suggesting that cluster formation was not occurring. The compounds for which photochemical cluster formation was observed had a disulfide bridge, and observed that breaking of the sulfur bridge also leads to oxidative addition reactions to alkenes.[13]

Earlier photochemical studies of **1** using ultrafast laser-flash photolysis with TRIR spectroscopy[19] were interpreted as indicating that excitation leads within 50 ps to two isomers of the CO dissociation product $Fe_2(\mu\text{-pdt})(CO)_5$, neither having a bridging carbonyl. Subsequent computational studies[20] were consistent with this assignment. Recent studies explored the coordination of the solvent in a species such as $Fe_2(\mu\text{-pdt})(CO)_5(Sol)$ using both spectral IR changes and DFT.[10] Hunt et al. showed that the solvent adducts were metastable and that IR difference spectra, generated by continuous-wave photolysis, displayed lower-frequency modes, consistent with a solvent adduct. We have observed this same behavior in acetonitrile and toluene.[6] In addition, we have measured the IR spectrum of the transient photoproduct(s) formed by 355 nm irradiation of **1** in a low-temperature (~100 K) alkane solution (methylcyclohexane; Figure S-7) and found it closely analogous to the TRIR spectrum measured by ultrafast TRIR spectroscopy.[19] Unsaturated metal carbonyls commonly form solvent complexes in alkane solution,[21] and this has now been established for $(\mu\text{-pdt})[Fe(CO)_3]_2$. In addition, the pattern of the back-reaction rates in solvents of varying coordination ability supports this solvent intermediate $Fe_2(\mu\text{-pdt})(CO)_5(Sol)$ as the predominant intermediate formed.

In summary, **1** undergoes CO labilization upon irradiation to give a solvent species, and this species reacts with CO to reform **1** under pseudo-first-order conditions. Second-order rate constants k_{CO} vary from 0.90 to 10^8 M^{-1} s^{-1}, and suggests that ligand substitution occurs by a dissociative type mechanism. In addition, $Fe_2(\mu\text{-pdt})(CO)_5(Sol)$ appears to undergo a competing reaction in aromatic solvents, to form another intermediate **I′**, which undergoes slow regeneration of **1** under excess CO. Because of the hydrogenase enzyme's structural and spectroscopic similarities[12] to **1**, we suggest that similar reactivity may be important for those circumstances where photoactivation plays a role in the enzyme's catalytic cycle. On-going studies are directed toward a more definitive characterization of the relevant intermediates.

■ ASSOCIATED CONTENT

Ⓢ Supporting Information

Experimental details, IR difference spectrum in THF, a plot of k_{obs} versus [CO] in THF monitored by IR, plots of residual absorbance in toluene versus [CO], plots of k_{obs} versus [CO] in hexanes and benzene, optical spectra before and after photolysis in toluene, and a low-temperature IR difference spectrum in methylcyclohexane. This material is available free of charge via the Internet at http://pubs.acs.org.

■ AUTHOR INFORMATION

Corresponding Author

*E-mail: works@sonoma.edu.

■ ACKNOWLEDGMENTS

These studies were partially supported by grants to P.C.F. and C.W. from the Chemistry Division of the National Science Foundation (Grants NSF-CHE-0749524 and NSF-CHE-1057808, respectively).

■ REFERENCES

(1) Adams, M. W. W. *J. Biol. Chem.* **1987**, *262*, 15054−15061.
(2) Adams, M. W. W. *Biochim. Biophys. Acta* **1990**, *1020*, 115−145.
(3) Thauer, R. K.; Kaufer, B.; Zahringer, M.; Jungermann, K. *Eur. J. Biol.* **1974**, *42*, 447−452.
(4) Lemon, B. J.; Peters, J. W. *J. Am. Chem. Soc.* **2000**, *122*, 3793−3794.
(5) Bennett, B.; Lemon, B. J.; Peters, J. W. *Biochemistry* **2000**, *39*, 7455−7460.
(6) Brown-McDonald, J.; Berg, S.; Peralto, M.; Works, C. *Inorg. Chim. Acta* **2009**, *362*, 318−324.
(7) Silakov, A.; Kamp, C.; Reijerge, E.; Happe, T.; Lubitz, W. *Biochemistry* **2009**, *48*, 7780−7786.
(8) Zhao, X.; Georgakaki, I. P.; Miller, M. L.; Mejia-Rodriguez, R.; Chiang, C.; Darensbourg, M. Y. *Inorg. Chem.* **2002**, *41*, 3917−3928.
(9) Thauer, R. K.; Kaufer, B.; Zahringer, M.; Jungermann, K. *Eur. J. Biochem.* **1974**, *42*, 477−452.
(10) Kaziannis, S.; Santabarbara, S.; Wright, J. A.; Greetham, G. M.; Towrie, M.; Parker, A. W.; Pickett, C. J.; Hunt, N. T. *J. Phys. Chem. B* **2010**, *114*, 15370−15379.
(11) Silaghi-Dumitrescu, I.; Bitterwolf, T. E.; King, R. B. *J. Am. Chem. Soc.* **2006**, *128*, 5342−5343.
(12) Galinato, M. G. I.; Whaldy, M. C.; Lehnert, N. *Inorg. Chem.* **2010**, *49*, 3201−3215.
(13) Kunkely, H.; Vogler, A. *J. Organomet. Chem.* **1998**, *568*, 291−293.
(14) Rimmer, R. D.; Richter, H.; Ford, P. C. *Inorg. Chem.* **2010**, *49*, 1180−1185.
(15) Motterlini, R.; Otterbein, L. E. *Nat. Rev. Drug Discovery* **2010**, *9*, 728−743.
(16) Mulder, D. W.; Shepard, E. M.; Meuser, J. E.; Joshi, N.; King, P. W.; Posewitz, M. C.; Broderick, J. B.; Peters, J. W. *Structure* **2011**, *19*, 1038−1052.
(17) The solubility of CO in THF was determined from 1 atm of CO pressure solubility as 0.0109 M (25°C). Payne, M. W.; Leussing, D. L.; Shore, S. G. *J. Am. Chem. Soc.* **1987**, *109*, 617−618.
(18) Westmeyer, M. D.; Galloway, C. P.; Rauchfuss, T. B. *Inorg. Chem.* **1994**, *33*, 4615−4616.
(19) Ridley, A. R.; Stewart, A. I.; Adamczyk, K.; Ghosh, H. N.; Kerkeni, B.; Guo, Z. X.; Nibbering, T. J.; Pickett, C. J.; Hunt, N. T. *Inorg. Chem.* **2008**, *47*, 7453−7455.
(20) Bertini, L.; Greco, C.; De Gioia, L.; Fantucci, P. *J. Phys. Chem. A* **2009**, *113*, 5657−5670.
(21) (a) Belt, S. T.; Ryba, D. W.; Ford, P. C. *Inorg. Chem.* **1990**, *29*, 3633−3634. (b) Hall, C.; Perutz, R. *Chem. Rev.* **1996**, *96*, 3125−3146.